

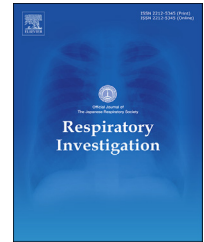


Since January 2020 Elsevier has created a COVID-19 resource centre with free information in English and Mandarin on the novel coronavirus COVID-19. The COVID-19 resource centre is hosted on Elsevier Connect, the company's public news and information website.

Elsevier hereby grants permission to make all its COVID-19-related research that is available on the COVID-19 resource centre - including this research content - immediately available in PubMed Central and other publicly funded repositories, such as the WHO COVID database with rights for unrestricted research re-use and analyses in any form or by any means with acknowledgement of the original source. These permissions are granted for free by Elsevier for as long as the COVID-19 resource centre remains active.

Available online at www.sciencedirect.com

Respiratory Investigation

journal homepage: www.elsevier.com/locate/resinv

Original article

Applicability of lung ultrasound in the assessment of COVID-19 pneumonia: Diagnostic accuracy and clinical correlations

Bianca Emilia Ciurba ^{a,b,1}, Hédi Katalin Sárközi ^{a,b,1},
István Adorjan Szabó ^{b,*}, Edith Simona Ianoși ^{a,b},
Bianca Liana Grigorescu ^{b,c}, Alpar Csipor-Fodor ^a, Toma P. Tudor ^d,
Gabriela Jimborean ^{a,b}

^a Pneumology Department from Mureș; County Clinical Hospital, Gheorghe Marinescu Street Number 5, Târgu Mureș, Postal code 540098, Romania

^b 'George Emil Palade' University of Medicine, Pharmacy, Science and Technology from Târgu Mureș, Gheorghe Marinescu Street Number 38, Postal code 540139, Romania

^c Anesthesiology and Intensive Therapy Department from Emergency Mureș; County Clinical Hospital, Gheorghe Marinescu Street Number 50, Târgu Mureș, Postal code 540136, Romania

^d University Hospital Lewisham & Greenwich, Owen Centre Lewisham Hospital Lewisham High Street, London SE13 6LH, UK

ARTICLE INFO

Article history:

Received 17 March 2022

Received in revised form

19 June 2022

Accepted 30 June 2022

Available online xxx

Keywords:

Lung ultrasound

COVID-19 pneumonia

Diagnostic accuracy

LUS score

Inflammation

ABSTRACT

Background: The purpose of this study was to assess the diagnostic accuracy of lung ultrasound (LUS) in determining the severity of coronavirus disease 2019 (COVID-19) pneumonia compared with thoracic computed tomography (CT) and establish the correlations between LUS score, inflammatory markers, and percutaneous oxygen saturation (SpO₂).

Methods: This prospective observational study, conducted at Târgu-Mureș Pulmonology Clinic included 78 patients with confirmed severe acute respiratory syndrome coronavirus-2 infection via nasopharyngeal real-time-polymerase chain reaction (RT-PCR) (30 were excluded). Enrolled patients underwent CT, LUS, and blood tests on admission. Lung involvement was evaluated in 16 thoracic areas, using AB₁ B₂ C (letters represent LUS pattern) scores ranging 0–48.

Results: LUS revealed bilateral B-lines (97.8%), pleural irregularities with thickening/discontinuity (75%), and subpleural consolidations (70.8%). Uncommon sonographic patterns were alveolar consolidations with bronchogram (33%) and pleural effusion (2%). LUS score cutoff values of ≤14 and > 22 predicted mild COVID-19 (sensitivity [Se] = 84.6%; area under the curve [AUC] = 0.72; P = 0.002) and severe COVID-19 (Se = 50%, specificity

Abbreviations: COVID-19, Coronavirus disease 2019; SARS-CoV-2, Severe acute respiratory syndrome coronavirus-2; LUS, Lung ultrasound; CT, Computed tomography; SpO₂, Percutaneous oxygen saturation; CRP, C-reactive protein; RT-PCR, Real-time-polymerase chain reaction; ARDS, Acute respiratory distress syndrome; ROC, Receiver Operating Characteristics; AUC, Area under the curve; NPV, Negative predictive value; PPV, Positive predictive value; ICC, Intraclass correlation coefficient.

* Corresponding authors. Szabó Adorjan István Republicii Street, nr 35, Ludus City, Postal code 545200, Mures County, Romania

E-mail address: sz.istvan.adorjan@gmail.com (I.A. Szabó).

¹ These authors share equal contribution as first authors.

<https://doi.org/10.1016/j.resinv.2022.06.015>

2212-5345/© 2022 The Japanese Respiratory Society. Published by Elsevier B.V. All rights reserved.

(Sp) = 91.2%, AUC = 0.69; $P = 0.02$), respectively, and values > 29 predicted the patients' transfer to the intensive care unit (Se = 80%, Sp = 97.7%). LUS score positively correlated with CT score ($r = 0.41$; $P = 0.003$) and increased with the decrease of SpO₂ ($r = -0.49$; $P = 0.003$), with lymphocytes decline ($r = -0.52$; $P = 0.0001$). Patients with consolidation patterns had higher ferritin and C-reactive protein than those with B-line patterns ($P = 0.01$; $P = 0.03$).

Conclusions: LUS is a useful, non-invasive and effective tool for diagnosis, monitoring evolution, and prognostic stratification of COVID-19 patients.

© 2022 The Japanese Respiratory Society. Published by Elsevier B.V. All rights reserved.

1. Introduction

In severe acute respiratory syndrome coronavirus-2 (SARS-CoV-2) infection, lung lesions develop before the onset of clinical symptoms, therefore, clinicians are searching for sensitive and specific imaging methods to detect incipient lung lesions associated with the infection. The World Health Organization (WHO) has recommended the use of chest imaging methods, especially when false-negative real-time-polymerase chain reaction (RT-PCR) results have been reported in patients with a high suspicion of coronavirus disease 2019 (COVID-19) [1]. Although thoracic computed-tomography (CT) is considered the gold standard for accurate assessment of lung lesions in COVID-19 [2], it is inappropriate for routine assessment due to the repeated irradiation and increased risk of cross-over contamination with SARS-CoV-2 during the investigation.

Lung ultrasound (LUS) has been introduced in international protocols for the diagnosis of respiratory diseases, especially in emergencies, and for the evaluation of pleural effusions. The first protocol using LUS in emergencies was described by Lichtenstein and Meziere, the BLUE protocol (Bedside Lung Ultrasound in Emergency) being the first to identify the cause of dyspnea and respiratory failure [3]. In recent decades, especially during the ongoing COVID-19 pandemic, LUS has gained renewed interest due to its many advantages: non-irradiating, repeatable method, performed quickly and efficiently at bedside due to portable devices, and cost-effectiveness. These advantages help the clinician in the triage of patients, in positive and differential diagnosis, disease stratification according to severity and prognosis, in evolution assessment (especially in severe patients with mechanical ventilation or complication), and monitoring of post-COVID lesions [4].

The present study aimed to highlight the applicability of LUS by describing characteristic LUS patterns in COVID-19 during evolution and to determine the diagnostic accuracy of LUS compared to chest CT based on the premise that LUS is non-inferior to thoracic CT. The primary outcome was to correlate COVID-19 pulmonary lesions assessed by LUS using an ultrasound score (A-B₁B₂C) compared to chest CT score and determine the diagnostic performance of LUS in comparison with thoracic CT. Secondary outcomes are represented by the detection of the correlations between LUS score and inflammatory markers (ferritin, C-reactive protein [CRP], fibrinogen

and D-dimers) and the correlation between LUS score and percutaneous oxygen saturation (SpO₂).

2. Materials and methods

A prospective cohort study, conducted at Târgu-Mureș Pulmonology Clinic, Mureș County Clinical Hospital, between January and March 2021, included 129 patients with suspected SARS-CoV-2 infection.

2.1. Ethical considerations

The members of the Local Ethics Commission of the Mureș County Clinical Hospital approved the development of the study in compliance with the patients' confidentiality clauses (No. approval 905/January 29, 2021). Informed consent was obtained from all subjects, according to the World Medical Association Declaration of Helsinki, revised in 2000, Edinburgh.

2.2. Patient characteristics and selection

Inclusion criteria were as follows: (1) patient age ≥ 18 years, (2) informed consent granted, and (3) confirmed diagnosis of SARS-CoV-2 infection by nasopharyngeal RT-PCR with a clinically active respiratory infection. The following exclusion criteria were applied: (1) denial of the patient to participate, (2) patients with negative or inconclusive RT-PCR test, and (3) patients with pre-existing comorbidities (pulmonary fibrosis, congestive heart failure). Patients were assessed three times during hospitalization: on "Admission" (first 24 h), "Control" (between the 4th and 5th day), and at "Discharge." During hospitalization, the patients underwent following investigations: chest CT, LUS, blood tests (cell blood count, inflammatory markers like ferritin, fibrinogen, CRP), and continuous monitoring of SpO₂ values with percutaneous pulse oximetry.

Disease severity types were assessed by symptoms, the need for oxygen and the CT lung involvement as follows: (1) mild forms: mildly symptomatic patient, without need for oxygen, with minimal chest CT changes (lung damage $< 25\%$); (2) moderate forms: dyspnea on moderate exertion, need for intermittent oxygen and pulmonary changes ranging between 25% and 50% of the lung surface; (3) severe forms: resting dyspnea, respiratory failure (tachypnea, intercostal

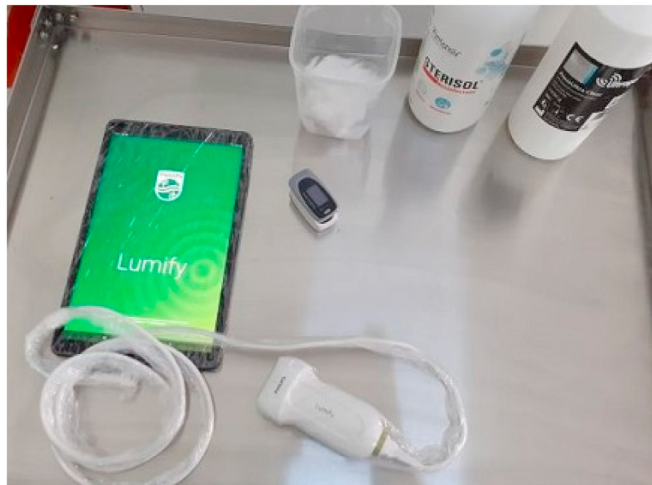


Fig. 1 – The portable Philips Lumify Ultrasound with linear transducer (covered with plastic foil, protecting the ultrasound machine when disinfected).

respiratory muscle traction), SpO₂ <93% at rest under oxygen with increased flow >6 L/min, and pulmonary changes involving >50% lung surface; and (4) critical forms: severe forms that required Intensive Care Unit admission, and mechanical ventilation due to acute respiratory distress syndrome (ARDS).

2.3. LUS examination

The LUS examinations were performed with Philips Lumify Ultrasound device (Philips South East Europe Office Oregon Park, District 2, Bucharest, Romania), with the high-frequency linear transducer L12-4 MHz (Fig. 1), and lung preset (gain 50–70 dB, scan depth 7–10 cm). During the examination, using the Lumify application, ultrasound recordings were stored to be analyzed outside the COVID area, by the performing resident physician (Level 2 operator: at least 20 supervised procedures and 200 non-supervised procedures) and validated by two doctors with certified competence in ultrasound (Level 3 operator: doctors with certified ultrasound proficiency).

A standard examination protocol was used, and 16 thoracic areas were evaluated following the division of the thorax by five anatomical lines: parasternal, anterior axillary, posterior axillary, scapular, and paravertebral. Each region was then divided into a superior and an inferior region [5].

Areas of LUS examination and examples of the complete scan are described in Table 1.

- L1, R1: between parasternal line and anterior axillary line in the superior left or right hemithorax
- L2, R2: between parasternal line and anterior axillary line in the inferior left or right hemithorax
- L3, R3: between anterior axillary and posterior axillary line in the superior left or right hemithorax
- L4, R4: between anterior axillary and posterior axillary line in the inferior left or right hemithorax
- L5, R5: between posterior axillary and scapular line in the superior left or right hemithorax
- L6, R6: between the posterior axillary and scapular line in the inferior left or right hemithorax
- L7, R7: between scapular and paravertebral line in the superior left or right hemithorax
- L8, R8: between scapular and paravertebral line in the inferior left or right hemithorax

LUS was performed with transducer using a transverse approach, and patient sitting at the edge of the bed, except for critically ill patients with non-invasive ventilation, who were examined in a supine position, tilted to the opposite side to visualize the posterior regions. An ultrasound score called AB₁B₂C was performed, each letter signifying the charact-

Table 1 – Regions of LUS examination and examples of the complete scan.

| | Posterior | Postero-lateral | Antero-lateral | Anterior | Anterior | Antero-lateral | Postero-lateral | Posterior |
|--|-----------|-----------------|----------------|----------|----------|----------------|-----------------|-----------|
| Superior | R7 | R5 | R3 | R1 | L1 | L3 | L5 | L7 |
| Inferior | R8 | R6 | R4 | R2 | L2 | L4 | L6 | L8 |
| R = right hemitorax, L = left hemitorax. | | | | | | | | |
| Superior | 3 | 2p | 1 | 0 | 1 | 2 | 1 | 0 |
| Inferior | 2p | 2 | 1 | 0 | 0 | 2p | 1 | 3 |

P: pleural involvement (thickening, disruption), quantified +1 point.

Total AB₁B₂C score: 21 + Nr. of pleural involvement (3 points) = 24 points.

Table 2 – AB₁B₂C LUS score.

| Severity Class | Score | Score Definition |
|--|-------|--|
| A | 0 | Normal pleural line, A-lines or less than 3 B-lines |
| B1 | 1 | >3 B-lines but their confluence is less than 50% of the lung surface |
| B2 | 2 | Confluent B-lines more than 50% of the lung surface |
| C | 3 | Subpleural or alveolar consolidation can be associated with aerial bronchogram |
| Pleural thickness or irregularities quantified +1 point. | | |

eristics of an ultrasound pattern, a score of 0–3 points for each thoracic quadrant, resulting in a total score of 0–48 points [5]. The AB₁B₂C score is detailed in Table 2. This score has clinical applicability and each performed ultrasound was quantified based on this score.

Findings were defined and recorded as follows [6,13]:

- A-lines are hyperechogenic artifacts, parallel with the pleural line, synchronous with respiratory movements, caused by the normally aerated lung.
- B-lines are hyperechoic, laser-beam-like, vertically (when using linear probe) or radially (with convex probe) oriented reverberation artifacts, which begin at the pleural line and extend to the bottom of the screen, without fading, synchronous with breathing movements.
- An interstitial syndrome is described as increased number of B-lines or confluent B-lines, with three or more B-lines in a longitudinal plane, in two or more scans. If the B-lines are focal (localized) the interstitial syndrome can be caused by interstitial pneumonia. When the B-lines are diffuse and bilateral, the interstitial syndrome can be caused by pulmonary edema/congestion, acute lung injury, or pulmonary fibrosis.
- If inflammatory process is present, the B-lines might be accompanied by pleural line irregularity or disruption, and appearance of small subpleural consolidations.
- Consolidation (hypoechoic area) can have a superficial distribution (below the pleural line) with small dimensions also called subpleural consolidation or non-translobar consolidations (in COVID-19 associated with high suspicion of micro-pulmonary infarction areas); or central/deep and large distribution also called translobar/alveolar consolidations appearing as “tissue-like” echogenic mass nearly echo density with the liver, with or without air bronchogram (hyperechogenic points).
- Pleural effusion is an anechoic (black) area between the parietal and visceral pleura.

2.4. Thoracic computed tomography (CT) examination

Patients included in the study underwent chest CT in the emergency department 24 h before hospitalization.

Non-contrast chest CT was performed with CT type Spiral Acquisition (SOMATOM Definition AS+, Siemens Healthcare,

Malvern, PA 19355, USA). The scans were acquired and reconstructed using the following parameters: 5–1 mm section thickness, 130 kV–100 kV, and tube current 35 mA. The mean CT dose index volume (CTDIvol) was 8.48 mGy. One senior radiologist from the emergency department performed and evaluated the chest CT of the COVID-19 patients, blinded to the clinical information. The radiologist assessed the percentage of the lobar damage, interpreting using the pulmonary window settings for the presence and distribution of the abnormalities. It was considered significant for COVID-19 pneumonia if ground-glass opacities with multilobar or patchy distribution, with or without interlobular septal thickening described as crazy paving pattern, or consolidation (parenchymal opacities obscuring the vessels), were present. After the senior radiologist assessed the lung damage involvement giving us a percentage of lung surface affected by significant COVID-19 lesions, then we used a CT severity score, a modified score based on the Total Severity Score (TSS) described by Li et al. [7]. CT severity score evaluation was based on summing up the significant COVID-19 pneumonia lesions involving all five lobes, assessed by a radiologist. After the radiologist described the lung damage involvement, it was scored as follows: no lung damage: score 0; 1%–15% damage: score 1; 16%–25% damage: score 2; 26%–50% damage: score 3; 51%–75% damage: score 4, and >76% damage: score 5. This semiquantitative scoring was modified by the standard CT score described by Pan et al. [8].

2.5. Statistical analysis

Descriptive analysis of the data was performed, and the continuous variables were expressed as mean \pm standard deviation (mean \pm SD) or median (interquartile ranges) due to the heterogeneity of the data. Inferential statistical analysis was performed with GraphPad Prism 8.0.1. (GraphPad Software Inc, San Diego, CA, USA) and MedCalc 20.009 Version (MedCalc Software Ltd, Ostend, Belgium). The normality of each variable was verified with the Kolmogorov–Smirnov test. When the normality of the data distribution was rejected, the statistical analysis was performed by non-parametric tests for paired (Wilcoxon test) or unpaired (Mann–Whitney) data. Reliability between LUS score interpretations by two doctors with ultrasound proficiency was determined by the intraclass correlation coefficient (ICC). ICC values were interpreted as poor (0.40–0.59), good (0.60–0.74), and excellent (0.75–1.0) [9]. The LUS score was compared with disease severity forms using single-factor ANOVA analysis (Friedman test). The Pearson correlation was used to analyze the correlation between LUS score and lymphocytes count, and the Spearman correlation was applied for LUS score and CT score, LUS score and SpO₂, LUS score and inflammatory markers. A correlation value > 0.7 was considered strong. Receiver operating characteristics (ROC) curve, area under the curve (AUC), sensitivity, negative predictive value (NPV), specificity, and positive predictive value (PPV) were calculated to illustrate the performance of LUS as a diagnostic method based on the cutoff value of the ultrasound score. All tests were interpreted against the significance threshold $\alpha = 0.05$ and the statistical significance was considered for p-value values less than or equal to the significance threshold ($P \leq 0.05$).

3. Results

Of all 129 patients hospitalized in the Pneumology Clinic from January to March 2021 with suspected SARS-CoV-2 infection, 78 patients with positive SARS-CoV-2 infection confirmed with RT-PCR swab test were initially enrolled. Fourteen patients met the exclusion criteria as thoracic CT was not performed, and 16 of them had comorbidities like acute cardiac failure and pulmonary fibrosis. The 48 patients finally enrolled included 27 (56%) males and 21 (44%) females, with a median age of 68 years. SpO₂ was decreased in all patients regardless of COVID-19 severity, 21 (44%) patients required medium flow oxygen therapy (4–6 L/min), 13 (27%) patients required a flow rate >6 L/min, and 14 (29%) patients did not require oxygen. The value of ferritin was increased in 38 patients (88%), the highest value was 7500 ng/mL, and 40 patients (89%) had elevated CRP, with a maximum value of 334.3 mg/L. Demographic data, clinical and paraclinical characteristics are detailed in Table 3.

All 48 patients presented with an interstitial syndrome characterized by B-line pattern, of which 89.5% (n = 43) of them presented with confluent (4–8 mm) B-lines, 31.2% converged to white lung sign (hyperechogenicity of entire screen), and only 12.5% (n = 5) patients presented with focal B-lines. The confluent and coalescent B-lines were distributed predominantly in posteroinferior regions (68.7%, n = 33 patients), in posterolateral regions (62.5%, n = 30 patients in left region; and 66.6%, n = 32 patients in right region), and only 33.3% (n = 16 patients) in superior regions.

Another characteristic pattern for COVID-19 was pleural irregularities with thickening and discontinuity (75%) associated with subpleural consolidations (70.8%). Less specific ultrasonographic patterns were alveolar consolidations and pleural effusions. The LUS patterns are described in Table 4 and Fig. 2.

The median LUS score at admission was 11 in mild, 15 in moderate-to-severe, and 26 in critical disease patients, which were significantly different ($P < 0.004$). LUS follow-up on the fourth day of hospitalization showed that the median LUS score increased from 15 to 20 points in severe form, and from 26 to 30 in critical form, without a statistical difference ($P = 0.17$), with the coalescence of B lines and lung consolidations in 20 patients (42%).

The ICC for LUS score was 0.996 (95% confidence interval [CI]: 0.994–0.998), using the two-way mixed effects model, where people effects are random and measures effects are fixed. For four patients, the thoracic CT did not reveal any pulmonary lesions on admission, even though they had positive RT-PCR test, and the LUS showed interstitial lesions (B-lines). Two patients had LUS score of 9 at admission, one patient had a score of 11, and one had a score of 14, even though thoracic CT did not reveal interstitial lesions. The comparative imaging characteristics between chest CT and LUS are presented in Fig. 3.

LUS had an increased diagnostic performance to detect mild forms of COVID-19 at a cutoff value of LUS score ≤ 14 , with sensitivity of 84.6%, with NPV of 91.7%, Specificity of 62.9%, with PPV of 45.8% (AUC = 0.72; Youden Index = 0.47; $P = 0.002$). ROC analysis showed that LUS scores >22 could

Table 3 – Demographic, clinical and paraclinical data.

| Clinical characteristics | All patients (n = 48) | COVID-19 severity forms | | | |
|---|-----------------------|-------------------------|-------------------|----------------|------------------|
| | | Mild (n = 13) | Moderate (n = 22) | Severe (n = 8) | Critical (n = 5) |
| Age | 68 | 71 | 65 | 65 | 77 |
| Sex | M 56%/F 44% | 4 M/9 F | 15 M/7 F | 3 M/5 F | 5 M/0 F |
| Body Mass Index | 28 | 26 | 29 | 30 | 30 |
| Smoking status | 15 (31.3%) | 4 (8.3%) | 6 (12.5%) | 4 (8.3%) | 1 (2.1%) |
| COPD/Asthma | 11 (22.9%) | 1 (2.1%) | 4 (8.3%) | 3 (6.3%) | 3 (6.3%) |
| Hypertension | 37 (77.1%) | 12 (25%) | 15 (31.3%) | 6 (12.5%) | 4 (8.3%) |
| Another CV diseases | 25 (52.1%) | 8 (16.7%) | 10 (20.8%) | 3 (6.3%) | 4 (8.3%) |
| Type II Diabetes | 21 (43.8%) | 4 (8.3%) | 11 (22.9%) | 2 (4.2%) | 4 (8.3%) |
| Renal Disease | 13 (27.1%) | 4 (8.3%) | 6 (12.5%) | 0 | 3 (6.3%) |
| Hepatic cytolysis | 16 (33.3%) | 4 (8.3%) | 8 (16.7%) | 2 (4.2%) | 2 (4.2%) |
| SpO ₂ (ambient air) | 89 | 93 | 90 | 88 | 81 |
| SpO ₂ (with O ₂) | 94 (n = 34) | 97 (n = 5) | 95 (n = 18) | 95 (n = 8) | 90 (n = 5) |
| LUS score (admission) | 14 (IQR: 2–35) | 11 (IQR: 2–16) | 15 (IQR:5–30) | 15 (IQR:11–31) | 26 (IQR:11–35) |
| LUS score (4–5 days after) | 15 (IQR: 3–33) | 10.5 (IQR:3–18) | 15 (IQR:3–29) | 20 (IQR:7–33) | 30 (IQR:15–32) |
| LUS score (discharge) | 10 (IQR:2–29) | 9 (IQR:5–12) | 9 (IQR: 2–28) | 18 (IQR:7–22) | — |
| CT (extension%) | 38 (IQR:0–75) | 14 | 40 | 56 | 63 |
| CT score | 3 (IQR: 0–5) | 2 | 3 | 4 | 4 |
| Mediastinal lymphadenopathy | 9 (18.8%) | 2 (4.2%) | 4 (8.3%) | 2 (4.2%) | 1 (2.1%) |
| Laboratory blood results | | | | | |
| *Ferritin (ng/mL) | 1321.9 ± 1424.5 | 967.9 ± 1120 | 1712.8 ± 1831.1 | 788.7 ± 283.9 | 1284 ± 717.3 |
| *Fibrinogen (mg/dL) | 458 ± 145 | 389.9 ± 102.4 | 507.7 ± 150.2 | 470.3 ± 163.4 | 440.6 ± 169.5 |
| *C-Reactive Protein (mg/L) | 85.7 ± 96.8 | 25.4 ± 37.7 | 116.9 ± 116.2 | 127.3 ± 66.5 | 20.5 ± 19.8 |
| ^a D-dimer (qualitative) | 20 (41.7%) | 1 (2.1%) | 12 (25%) | 4 (8.3%) | 3 (6.3%) |
| *Lymphocytes (%) | 13.6 ± 8.9 | 19.6 ± 10.5 | 11.4 ± 7.4 | 13.7 ± 6.2 | 7 ± 6.5 |

IQR: interquartile range; *mean ± Standard Deviation; M: male; F: female; CV: cardio-vascular, n: number of patients.

^a Qualitative analyses: number of patients with positive D-Dimer.

Table 4 – LUS and CT patterns in COVID-19: Distribution and localization.

| LUS patterns in COVID-19 | | Thoracic CT patterns in COVID-19 | |
|---|----------------|---|-----------------|
| Interstitial syndrome | 48 (100%) | Interstitial syndrome | 39 (81.3%) |
| - Focal B-lines (1–3 mm) | 5 (12.5%) | - Ground Glass Opacities (GGO) | 33 (68.8%) |
| - Confluent B-lines (4–8 mm) | 43 (89.5%) | - Interstitial infiltration | 12 (25%) |
| - “White lung” sign | 15 (31.2%) | - Crazy paving pattern | 3 (6.3%) |
| Unilateral | 3 (6.3%) | Unilateral | 7 (14.6%) |
| Bilateral, patchy and diffuse | 45 (93.8%) | Bilateral | 36 (75%) |
| Distribution: | Affected zones | Distribution: | Affected zones: |
| Superior | 60 | Superior | 11 |
| Anterior | 43 | Anterior | 0 |
| Lateral | 64 | Lateral | 0 |
| Posterolateral | 106 | Posterolateral | 9 |
| Posteroinferior | 62 | Posteroinferior | 19 |
| Subpleural consolidations | 34 (70.8%) | Subpleural consolidations | 9 (18.8%) |
| Unilateral | 11 (22.9%) | Unilateral | 9 (18.8%) |
| Bilateral | 23 (47.9%) | Bilateral | 0 |
| Distribution: | Affected zones | Distribution: | Affected zones: |
| Superior | 17 | Superior | 0 |
| Lateral | 15 | Lateral | 0 |
| Posterolateral | 41 | Posterolateral | 4 |
| Posteroinferior | 21 | Posteroinferior | 5 |
| Alveolar consolidations with bronchogram | 16 (33.3%) | Alveolar consolidations with bronchogram | 2 (4.2%) |
| Unilateral | 12 (25%) | Unilateral | 2 (4.2%) |
| Bilateral | 4 (8.3%) | Bilateral | 0 |
| Distribution: | Affected zones | Distribution: | Affected zones: |
| Lateral | 3 | Lateral | 1 |
| Posterolateral | 9 | Posterolateral | 1 |
| Posteroinferior | 4 | Posteroinferior | 0 |
| Pleural effusion | 1 (2.1%) | Pleural effusion | 2 (4.2%) |
| Unilateral (quad sign) | 1 (2.1%) | Unilateral | 2 (4.2%) |
| Bilateral | 0 | Bilateral | 0 |
| Pleural irregularities (thickening, discontinuity) | 36 (75%) | Pleural thickening | 4 (8.3%) |
| Unilateral | 9 (18.8%) | Unilateral | NS |
| Bilateral | 27 (56.3%) | Bilateral | NS |
| | | Mediastinal lymphadenopathy | 9 (18.8%) |

NS: not specified.

detect severe COVID-19, with a sensitivity of 50% with NPV = 79.5% and specificity of 91.2% with PPV = 66.7% (AUC = 0.69; Youden Index = 0.35; $P = 0.02$). A cutoff value of LUS score >29 predicts the patients' transfer to the ICU with a sensitivity of 80% (95% CI: 28.4–99.5) and a specificity of 97.7% (95% CI: 87.7–99.9; AUC = 0.89; $P < 0.001$). The ROC curve for LUS score is represented in Fig. 4, using the MedCalc 20.009 Version graphic.

Spearman correlation analysis revealed a moderate positive correlation between LUS score and CT score ($r = 0.41$; 95% CI: 0.14–0.63; $P = 0.003$), moderate correlation between LUS score and SpO₂ decrease on admission ($r = -0.49$; 95% CI: 0.68 to -0.23; $P = 0.003$). The presence of a statistically significant correlation was observed between the LUS score and the number of lymphocytes ($r = -0.52$; 95% CI -0.70 to -0.27; $P = 0.0001$), together with the increase in the LUS score resulting in accentuation of lymphopenia. The correlation between LUS score and ferritin ($r = 0.11$, 95% CI -0.19 to 0.41; $P = 0.45$) as well as between LUS score and fibrinogen ($r = 0.26$, 95% CI: 0.09 to 0.55; $P = 0.14$) was not statistically significant. Nevertheless, patients with consolidation pattern had significant higher ferritin ($P = 0.016$;

median: 1031 ng/mL) and CRP ($P = 0.03$; mean: 108 ± 95 mg/dL) values compared to the group only with B-lines (median: 628.05 ng/mL; mean: 44.6 ± 97.9 mg/dL). No statistically significant positive correlations were observed between the LUS score and other laboratory parameters (D-dimers or fibrinogen).

4. Discussions

LUS has been evaluated in clinical trials and included in diagnostic protocols for multiple respiratory pathologies. Ultrasound showed an increased specificity and sensitivity in the diagnosis of pneumothorax [10,11], and it can reach 75%–90% specificity and 85%–95% sensitivity for pneumonia detection [12]. LUS is superior to conventional chest radiography in detecting or excluding pulmonary edema [13]. Sonographic signs of COVID-19 are similar to those of other viral types of pneumonia [14]. There is no evidence for a pathognomonic ultrasound sign for COVID-19, but the literature has observed that certain ultrasound patterns such as B-lines with bilateral distribution, pleural irregularity, and

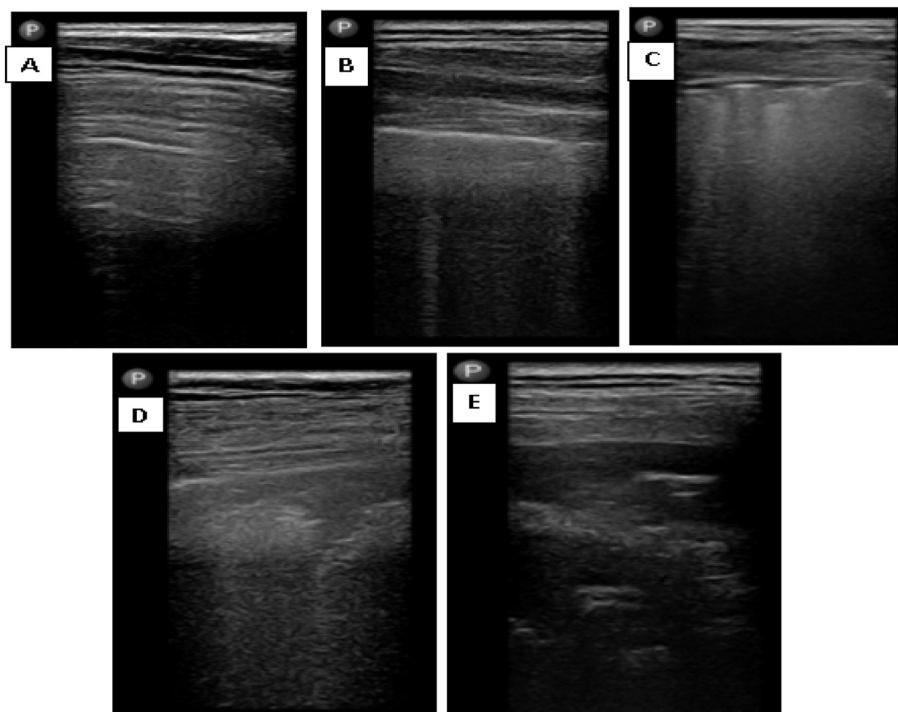


Fig. 2 – Ultrasound patterns in COVID-19. (A) Score 0: horizontal A-lines; (B) Score 1: B-lines <50% of surface; (C) Score 2: coalescent B-lines >50% of surface; (D) Score 3: subpleural consolidation “shred sign”; (E) Score 3: alveolar consolidation with bronchogram.

subpleural consolidations, lead to increased suspicion of COVID-19 in a pandemic and clinical context [15].

In most observational studies, the main sonographic sign observed in an increased proportion of patients with COVID-19 was B-lines. There are multiple varieties of B-lines, such as focal, which presents in the initial stage of the disease, multifocal, separate, or coalescent B-lines. In a cohort of 105 COVID-19 patients, 92% of the patients had confluent B-lines and 38% had a “white lung” sign [16]. LUS shows high sensitivity and specificity in the detection of B-lines [17,18]. The observations of the present study are consistent with those in the literature as patients in all study presented with B-lines, with predominantly bilateral distribution (93.8%). Another sonographic sign described in the present study with a higher prevalence (70.8%) was subpleural consolidations. More extensive subpleural consolidations were observed in critically ill COVID-19 patients with infected posterolateral thoracic regions in the mechanically-invasive ventilated group [19]. Lichter et al. [20] reported that 77.5% of patients had subpleural consolidations, while in another cohort subpleural consolidations were found in 6 of 22 patients [21]. An uncommon pattern was deep alveolar consolidations, detected in 50% of patients, with the dynamic bronchogram sign [22]. In the present study, we report 33% prevalence, with the majority (25%) having unilateral distribution. An extremely rare sign is the presence of pleural effusion [23], which is consistent with our findings, with only one case of minimal pleural effusion. “HighLUS” pattern was accurate in predicting RT-PCR outcomes in patients with suspected SARS-CoV-2 infection. This pattern consists of

bilateral and multifocal clusters of separate or coalescent B-lines, large hyperechoic bands (called “light beams”), multifocal peripheral consolidations, regular and irregular pleural lines, with or without large consolidations [24].

The results of the present study showed that the severity of SARS-CoV-2 pneumonia assessed by LUS is strongly associated with severity as assessed by chest CT. Therefore, ultrasound could replace chest CT for initial assessment as well as monitoring the evolution of lung damage in symptomatic patients with confirmed SARS-CoV-2 infection. The correlation between LUS and CT scores was moderate, although no abnormal CT results were marked as normal on ultrasound. On the contrary, four patients were identified with minimal lesions on ultrasound but no changes on chest CT. An excellent correlation between CT and ultrasound, the presence of confluent B-lines corresponding to “ground-glass opacities” has been reported [25]. A comparative study between LUS and chest CT in assessing the severity of COVID-19 pneumonia in a cohort of 100 patients confirmed with SARS-CoV-2 found that the LUS score was significantly associated with chest CT severity scan and a cutoff value < 13 excluded severe SARS-CoV-2 pneumonia with >90% sensitivity [26]. Our results are consistent with those in the literature, LUS showed an increased diagnostic performance in detecting mild COVID-19 forms at a cutoff value of ≤ 14 , with 84.62% sensitivity, and severe COVID-19 forms at a cutoff value of >22 with a specificity of 91.18%. Studies have found that ultrasound scores indicate critical evolution [27]. Our study showed that LUS scores >29 is predictive of patients’ transfer to the ICU, with a sensitivity of 80% and a specificity of 97.7%.

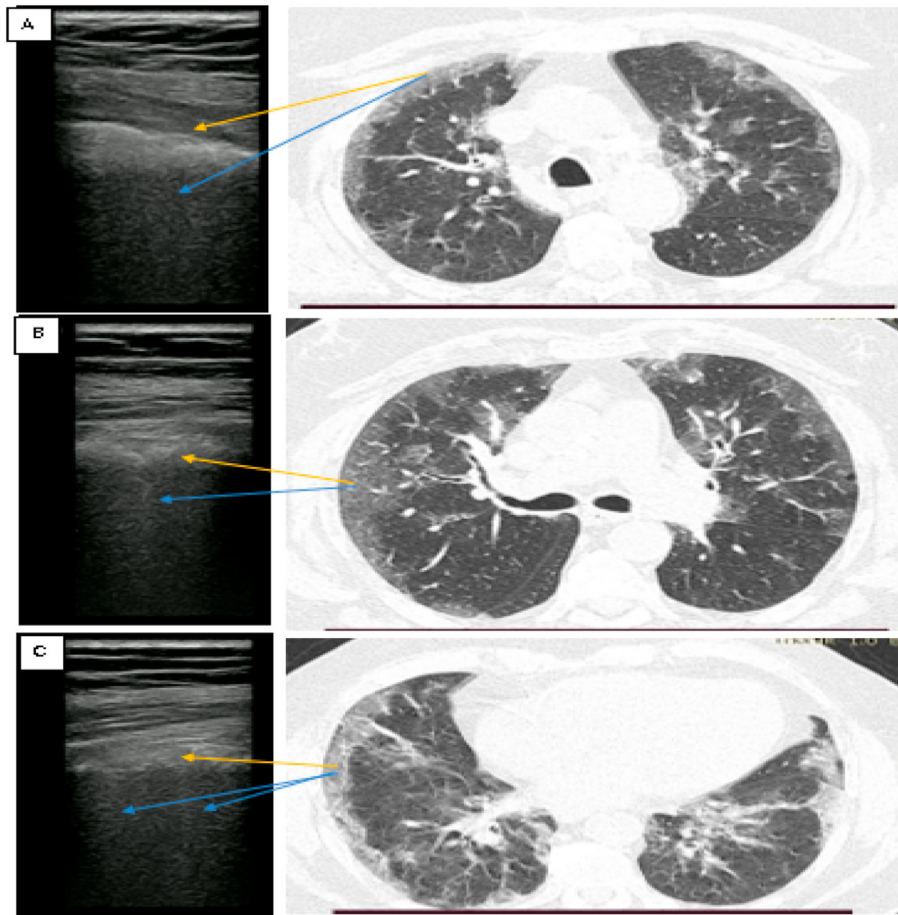


Fig. 3 – Comparative LUS and CT in COVID-19 patients. Yellow arrow = pleural line with irregularities and discontinuity (A), subpleural consolidation (B, C). Blue arrow = multiple B-lines with coalescence tendency. (For interpretation of the references to colour in this figure legend, the reader is referred to the Web version of this article.)

Secco et al. have shown that patients with SARS-CoV-2 infection with consolidation ultrasound pattern have a worse 30-day prognosis than those with an interstitial pattern (B lines) or no lung changes [28]. Laboratory parameters currently determined in SARS-CoV-2 infection are related to

the clinical course of the infection with a more severe evolution in patients with elevated levels of ferritin [29]. Elevated CRP and LDH levels were correlated with the extension of pneumonia quantified by chest CT [30,31]. In the present study, elevated CRP and ferritin levels can be considered

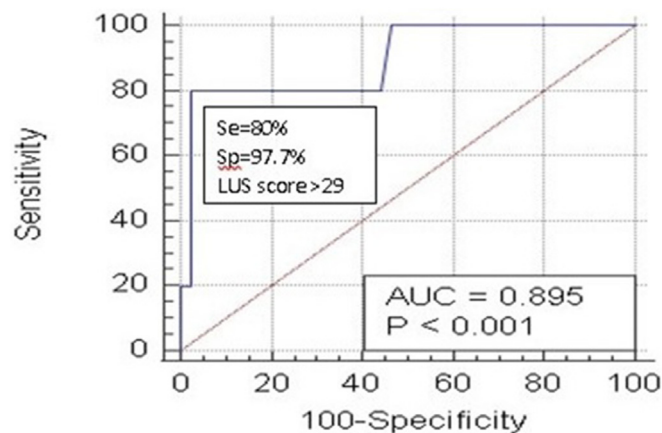


Fig. 4 – The Receiver Operating Characteristic (ROC) Curve for LUS score. The area under the curve (AUC): 89.5%, indicates the transfer to the Intensive Care Unit. Red line: reference line; Blue line: LUS Score. (For interpretation of the references to colour in this figure legend, the reader is referred to the Web version of this article.)

prognostic factors for disease severity, given that significantly higher values of inflammatory markers were detected in the group with consolidation pattern compared with the group of patients without consolidation on LUS.

The present study had some limitations. First, it was an short term, observational study without randomization or blinding design. In addition, the relatively small sample size of the cohort was a limitation, but the cohort was representative (we excluded the pathology that interferes with a false positive LUS image pattern) and the chance of selection bias was minimal. The main limitation of the study was the lack of a convex transducer that allowed better visualization of the depth of lesions with central distribution, especially useful for patients with obesity. The linear transducer used has a better frequency, ranging 4–12 MHz, and can scan also deeper or central lesions, by optimization of the depth of field view to 9 cm; adjusting the transducer focal zone to the level of the pleural line for increased spatial resolution. As the central distribution was not characteristic of chest CT and LUS evaluation, we consider that the results of the present study were not heavily influenced. As seen in Table 3, the alveolar consolidations with a deeper/central distribution were better observed by LUS in comparison with CT because of the air bronchogram sign (hyperechoic points in the hypoechoic consolidation) and because LUS was performed in evolution on 4th or 5th day of hospitalization when cytokine storm or bacterial suprainfection was probably high. The convex probe can underestimate the thickening of the pleural line was also a reason for choosing the linear probe.

The strength of the present study was the comprehensive examination of 16 chest areas, compared to other studies that used standard protocol with scoring proposed by Soldati et al. which had a different scanning approach for 14 intercostal thoracic areas [32]. The LUS images were validated by two medical doctors with certified US proficiency who were blinded to the patients' medical history.

5. Conclusions

LUS represents a useful, non-invasive and effective tool for diagnosis, monitoring evolution, and prognostic stratification of COVID-19 patients. The LUS score was associated with disease severity and clinical features. LUS had good diagnostic accuracy, highlighted by higher sensitivity and specificity in the detection of COVID-19 severity types and predicting the ICU transfer of critical patients. LUS could replace chest CT for initial assessment as well as monitoring the evolution of lung damage in patients confirmed with SARS-CoV-2 infection. LUS integration into the clinical management of COVID-19 is strongly recommended.

Conflict of Interest

Ciurba Emilia Bianca, Sárközi Katalin Hédi, Szabó Adorjan István, Ianoși Simona Edith, Grigorescu Liana Bianca, Csipor-Fodor Alpar, Toma Tudor, Jimborean Gabriela received the portable Philips Lumify Ultrasound with linear transducer during the study period from Philips Medical System (Philips

South East Europe Office Oregon Park, District 2, Bucharest, Romania) and declare no other conflict of interest including stock ownership, honoraria, travel fees, manuscript or licensing fees, endowed departments by commercial entitles subsidies or donation.

Acknowledgments

The authors thank Philips Medical Systems (Philips South East Europe Office Oregon Park, District 2, Bucharest, Romania), which provided the Philips Lumify Ultrasound with the linear transducer.

REFERENCES

- [1] Geneva: World Health Organization. Use of chest imaging in COVID-19: a rapid advice guide. World Health Organization Collaborative Group; 2020. WHO/2019-nCoV/Clinical/Radiology_imaging/2020.1). Licence: CC BY-NC-SA 3.0 IGO, https://apps.who.int/iris/bitstream/handle/10665/332336/WHO-2019-nCoV-Clinical-Radiology_imaging-2020.1-eng.pdf?sequence=1&isAllowed=y.
- [2] Ravikanth R. Diagnostic accuracy and false-positive rate of chest CT as compared to RT-PCR in coronavirus disease 2019 (COVID-19) pneumonia: a prospective cohort of 612 cases from India and review of literature. *Indian J Radiol Imag* 2021;31:161–9.
- [3] Lichtenstein DA, Meziere GA. Relevance of lung ultrasound in the diagnosis of acute respiratory failure, the BLUE protocol. *Chest* 2008;134:117–25.
- [4] Wang M, Luo X, Wang L, Estill J, Lv M, Zhu Y, et al. A comparison of lung ultrasound and computed tomography in the diagnosis of patients with COVID-19: a systematic review and meta-analysis. *Diagnostics* 2021;11(8):1351. <https://doi.org/10.3390/diagnostics11081351>.
- [5] Szabo IA, Agoston G, Varga A, Cotoi OS, Frigy A. Pathophysiological background and clinical practice of lung ultrasound in COVID-19 patients: a short review. *Anatol J Cardiol* 2020;24:76–80.
- [6] Jimborean G, Ianoși ES, Nemeș RM, Toma TP. Basic thoracic ultrasound for the respiratory physician. *Pneumologia* 2015;64(3):12–8. PMID: 26738366.
- [7] Li K, Fang Y, Li W, Pan C, Qin P, Zhong Y, et al. CT image visual quantitative evaluation and clinical classification of coronavirus disease (COVID-19). *Eur Radiol* 2020;30(8):4407–16. <https://doi.org/10.1007/s00330-020-06817-6>.
- [8] Pan F, Ye T, Sun P, Gui S, Liang B, Li L, et al. Time course of lung changes at chest CT during recovery from coronavirus disease 2019 (COVID-19). *Radiology* 2020;295(3):715–21. <https://doi.org/10.1148/radiol.2020200370>.
- [9] Hallgren KA. Computing inter-rater reliability for observational data: an overview and tutorial. *Tutor. Quant. Methods Psychol.* 2012;8(1):23–34. <https://doi.org/10.20982/tqmp.08.1.p023>.
- [10] Staub LJ, Biscaro RRM, Kaszubowski E, Maurici R. Chest ultrasonography for the emergency diagnosis of traumatic pneumothorax and haemothorax: a systematic review and meta-analysis. *Injury* 2018;49:457–66.
- [11] Alrajhi K, Woo MY, Vaillancourt C. Test characteristics of ultrasonography for the detection of pneumothorax: a systematic review and meta-analysis. *Chest* 2012;141:703–8.

- [12] Staub LJ, Mazzali Biscaro RR, Kaszubowski E, Maurici R. Lung ultrasound for the emergency diagnosis of pneumonia, acute heart failure, and exacerbations of chronic obstructive pulmonary disease/asthma in adults: a systematic review and meta-analysis. *J Emerg Med* 2019;56:53–69.
- [13] Volpicelli G, Elbarbary M, Blaivas M, Lichtenstein DA, Mathis G, Kirkpatrick AW, et al. International evidence-based recommendations for point-of-care lung ultrasound. *Intensive Care Med* 2012;38:577–91.
- [14] Tsung JW, Kessler DO, Shah VP. Prospective application of clinician performed lung ultrasonography during the 2009 H1N1 influenza pandemic: distinguishing viral from bacterial pneumonia. *Crit Ultrasound J* 2012;4: 16–0.
- [15] Schmid B, Feuerstein D, Lang CN, Fink K, Steger R, Rieder M, et al. Lung ultrasound in the emergency department - a valuable tool in the management of patients presenting with respiratory symptoms during the SARS-CoV-2 pandemic. *BMC Emerg Med* 2020;20:96.
- [16] Yasukawa K, Minami T, Boulware D, Shimada A, Fischer EA. Point-of-Care lung ultrasound for COVID-19: findings and prognostic implications from 105 consecutive patient. *J Intensive Care Med* 2021;36:334–42.
- [17] Favot M, Malik A, Rowland J, Haber B, Ehrman R, Harrison N. Point-of-Care lung ultrasound for detecting severe presentations of coronavirus disease 2019 in the emergency department: a retrospective analysis. *Crit Care Explor* 2020;2:e0176.
- [18] Peyrony O, Marbeuf-Gueye C, Truong V, Giroud M, Rivière C, Khenissi K, et al. Accuracy of emergency department clinical findings for diagnosis of coronavirus disease 2019. *Ann Emerg Med* 2020;76:405–12.
- [19] Seiler C, Klingberg C, Hardstedt M. Lung ultrasound for identification of patients requiring invasive mechanical ventilation in COVID-19. *J Ultrasound Med* 2021;9999:1–13.
- [20] Lichter Y, Topilsky Y, Taieb P, Banai A, Hochstadt A, Merdler I, et al. Lung ultrasound predicts clinical course and outcomes in COVID-19 patients. *Intensive Care Med* 2020;46:1873–83.
- [21] Lomoro P, Verde F, Zerboni F, Simonetti I, Borghi C, Fachinetti C, et al. COVID-19 pneumonia manifestations at the admission on chest ultrasound, radiographs, and CT: single-center study and comprehensive radiologic literature review. *Eur J Radiol Open* 2020;7:100231.
- [22] Nouvenne A, Zani MD, Milanese G, Parise A, Baciarello M, Bignami EG, et al. Lung ultrasound in COVID-19 pneumonia: correlations with chest CT on hospital admission. *Respiration* 2020;99:617–24.
- [23] Sahu AK, Mathew R, Bhoi S, Sinha TP, Nayer J, Aggarwal P. Lung sonographic findings in COVID-19 patients. *Am J Emerg Med* 2021;45:324–8.
- [24] Volpicelli G, Gargani L, Perlina S, Spinelli S, Barbieri G, Lanotte A, et al. Lung ultrasound for the early diagnosis of COVID-19 pneumonia: an international multicenter study. *Intensive Care Med* 2021b;47:444–54.
- [25] Tung-Chen Y, Martí de Gracia M, Díez-Tascón A, Alonso-González R, Agudo-Fernández S, Parra-Gordo ML, et al. Correlation between chest computed tomography and lung ultrasonography in patients with coronavirus disease 2019 (COVID-19). *Ultrasound Med Biol* 2020;46:2918–26.
- [26] Zieleskiewicz L, Markarian T, Lopez A, Taguet C, Mohammadi N, Boucekine M, et al. Comparative study of lung ultrasound and chest computed tomography scan in the assessment of severity of confirmed COVID-19 pneumonia. *Intensive Care Med* 2020;46:1707–13.
- [27] Rubio-Gracia J, Giménez-López I, Garcés-Horna V, López-Delgado D, Sierra-Monzón JL, Martínez-Lostao L, et al. Point-of-care lung ultrasound assessment for risk stratification and therapy guiding in COVID-19 patients: a prospective noninterventional study. *Eur Respir J* 2021;58:2004283.
- [28] Secco G, Delorenzo M, Salinaro F, Zattera C, Barcella B, Resta F, et al. Lung ultrasound presentation of COVID-19 patients: phenotypes and correlations. *Intern Emerg Med* 2021;16:1317–27.
- [29] Henry BM, de Oliveira MHS, Benoit S, Plebani M, Lippi G. Hematologic, biochemical and immune biomarker abnormalities associated with severe illness and mortality in coronavirus disease 2019 (COVID-19): a meta-analysis. *Clin Chem Lab Med* 2020;58:1021–8.
- [30] Liu T, Zhang J, Yang Y, Ma H, Li Z, Zhang J, et al. The role of interleukin-6 in monitoring severe case of coronavirus disease 2019. *EMBO Mol Med* 2020;12:e12421.
- [31] Xiong Y, Sun D, Liu Y, Fan Y, Zhao L, Li X, et al. Clinical and high-resolution CT features of the COVID-19 infection: comparison of the initial and follow-up changes. *Invest Radiol* 2020;55:332–9.
- [32] Soldati G, Smargiassi A, Inchingolo R, Buonsenso D, Perrone T, Briganti DF, et al. Proposal for international standardization of the use of lung ultrasound for patients with COVID-19: a simple, quantitative, reproducible method. *J Ultrasound Med* 2020;39:1413–9.